J. Phys. D: Appl. Phys. **23** (1990) 682–685. Printed in the UK

A double layer induced ionisation instability

James C Johnson, Nicola D'Angelo and Robert L Merlino

Department of Physics and Astronomy, The University of Iowa, Iowa City, Iowa 52242-1479, USA

Received 23 October 1989, in final form December 1989

Abstract. Low-frequency (~500–~2000 Hz) oscillations are detected in a double-plasma device in association with double layers in which the potential drop somewhat exceeds the ionisation potential of the gas. The oscillations are interpreted as ion-acoustic waves excited by an ionisation instability. A simple theory of the instability is presented and its results are compared with observations.

1. Introduction

In the course of our investigation of double layers produced by ion injection into the target chamber of a double-plasma (DP) device (Johnson *et al* 1989), we have observed that, under special circumstances to be discussed below, low-frequency (~500–~2000 Hz) waves may be spontaneously excited. These waves have the general features of ordinary ion-acoustic waves. Their excitation is related to the presence of a double layer having a potential drop, V_0, somewhat larger than the ionisation potential of the gas used in the device.

A brief description of the experimental set-up is given in § 2. For a more detailed account the reader is referred to Johnson *et al* (1989). In § 3 we present the main features of the self-excited waves, with particular regard to the conditions under which excitation takes place. In § 4 we describe an ionisation instability which seems to account for most of the observations. § 5 presents a discussion of the results and the conclusions.

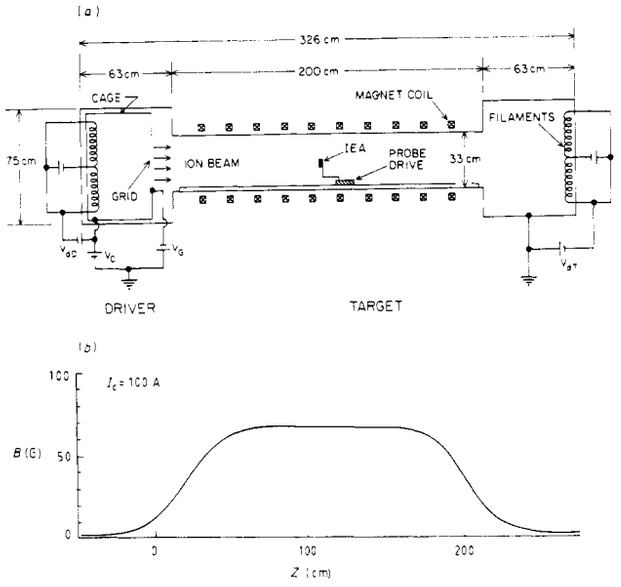

Figure 1. (*a*) Schematic diagram of the experimental set-up. (*b*) Axial magnetic field profile.

2. Experimental set-up

The experiments were performed in the double-plasma (DP) device described by Johnson *et al* (1989). A schematic diagram is shown in figure 1(*a*). The central portion of the device consists of an aluminium tube 200 cm long and 33 cm in diameter and is provided, by means of a set of 10 coils, with a longitudinal magnetic field of up to ~100 G. An axial magnetic field profile is shown in figure 1(*b*). Plasma is produced by discharges in noble gases in the two end chambers which are each 63 cm long and 75 cm in diameter. The device is divided into 'driver' and 'target' chambers by a large grid located near one end of the central chamber. The grid is generally biased at −75 V, so that electrons from either chamber cannot enter into the other. The potential of the driver chamber can be raised to ~100 V above that of the target chamber, thus allowing the injection of an ion beam from the driver into the target. Under appropriate conditions a stable double layer (DL) forms near the middle of the device (Johnson *et al* 1989).

The diagnostic tools used in our experiments are Langmuir probes, emissive probes and gridded ion-energy analysers. The gases which have been studied in the present investigations are He, Ne, Ar, Kr and Xe. In general, the experiments were performed in the pressure range $\sim 1 \times 10^{-3}$–$\sim 1 \times 10^{-2}$ Torr. We note

0022-3727/90/060682 + 04 $03.50

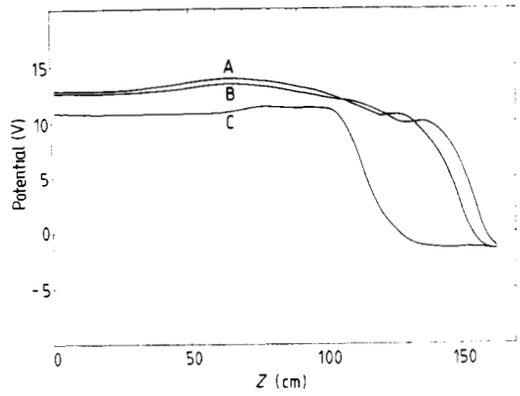

Figure 2. Axial profiles of the plasma potential obtained with the emissive probe at an argon pressure of 2×10^{-3} Torr. With profiles A and B the observed oscillation frequency is $f = 1.9$ kHz. No oscillation is present with profile C.

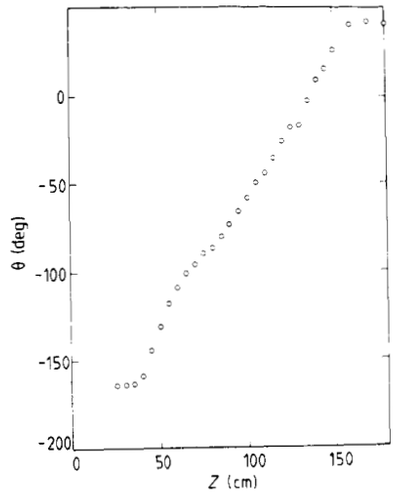

Figure 3. Phase against axial distance for a wave in argon at a pressure $p = 2 \times 10^{-3}$ Torr. The wave frequency is 1.3 kHz.

here that at these high pressures the ion beam injected from the driver into the target does not survive for long after crossing the grid separating the chambers since the mean free path for charge exchange of the beam ions with the neutral gas atoms is of the order of centimetres. Thus, several centimetres away from the grid into the target, the only ions present are 'thermal' ions. Their density varies along the axis of the device and it is of the order of $\sim 10^8\,\mathrm{cm}^{-3}$ near the grid. On the other hand, the energetic electrons (15–20 eV) produced by the DLs (see § 3) have mean free paths comparable to the distance between the DL and the grid separating driver and target.

3. Observations

Figure 2 shows three profiles of the plasma potential against axial distance away from the grid separating driver and target, for an argon pressure of 2×10^{-3} Torr. By small variations of either the magnetic field ($\Delta B \approx 3$ G) or the discharge currents ($\Delta I \approx 0.5$ A) in the driver and/or target, it was possible to change the potential profiles from either of the top two traces to the lower trace. These potential profiles were obtained by using an emissive probe, consisting of a 25 μm diameter, 0.7 cm long tungsten wire heated by a voltage of 1.7 V. The potential drop, V_0, across the DL for traces A and B was just above the argon ionisation potential, while V_0 for trace C was somewhat below it. Under conditions A and B narrowband low-frequency oscillations with $f = 1.9$ kHz were observed over the region between the grid and the DL potential transition with a peak amplitude of ~ 0.1 V ($e\tilde{\phi}/\kappa T_e \sim 10\%$), whereas no oscillation was present in case C. We were able to observe repeatedly, in many other instances, that similar low-frequency oscillations could be produced only when the potential drop across the associated double layer was larger than the gas ionisation potential.

A second observation refers to the pressure range in which the oscillations were found. In all cases investigated, considerations of device performance required the gas pressure not to exceed $\sim 1 \times 10^{-2}$ Torr. In argon the oscillations were detected in the pressure range $\sim 1 \times 10^{-3}$ to $\sim 1 \times 10^{-2}$ Torr; in krypton in the range $\sim 5 \times 10^{-4}$ to $\sim 1 \times 10^{-2}$ Torr; in xenon from $\sim 3 \times 10^{-4}$ to $\sim 1 \times 10^{-2}$ Torr. The waves were most easily excited in xenon, while in krypton about as easily as in argon. On the other hand, we were never able to observe them in neon or helium, in spite of the fact that DLs with V_0 exceeding the respective ionisation potentials were also present with these gases.

We also studied the propagation properties of these low-frequency waves. Propagation was found to be predominantly axial, as shown by a plot (figure 3) of the phase for a wave in argon, at $p = 2 \times 10^{-3}$ Torr, as a function of the axial displacement from the grid. The wave was detected as an oscillation in the floating potential of the moveable emissive probe. The reference for the phase measurements was provided by the signal from a Langmuir probe located near the axis, approximately 37 cm from the grid separating driver and target. The axial wavelength in this case appears to be $\lambda \approx 230$ cm. Thus, with a wave frequency $f = 1.3$ kHz one finds a phase velocity of $\sim 3 \times 10^5\,\mathrm{cm\,s}^{-1}$, comparable to the ion-acoustic speed. This type of result was common to practically all of the low-frequency wave observations.

A concise summary of our findings may be described as follows:

(i) the waves have the general features of low-frequency ion-acoustic waves ($f \approx 500$–2000 Hz) and peak amplitudes of ~ 0.1 V;

(ii) they are excited only when the gas pressure is relatively large;

(iii) excitation requires the presence of a DL with a voltage drop, V_0, somewhat above the ionisation potential of the gas;

(iv) the waves are most easily excited in a xenon gas, and also easily enough in krypton and argon. We have never observed them in either neon or helium.

4. The ionisation instability

We discuss in this section a mechanism by which ion-acoustic waves can be excited in a plasma with a low degree of ionisation, when electrons are present which are sufficiently energetic to ionise the neutral gas. In our DP device, the region between the grid and the position of the double layer ($0 \leqslant z \leqslant 150$ cm in figure 1) has a flux of energetic electrons which satisfy the above condition if V_0 is larger than the ionisation potential of the gas.

The manner in which ionisation can produce growth of ion-acoustic waves is easily visualised. Suppose an ion-acoustic perturbation of very small amplitude is present in the plasma. Regions corresponding to the crests of the wave (higher plasma density) are also regions of higher potential. If the ionising electrons have an energy just above the ionisation threshold, the ionisation cross section is a rapidly increasing function of the electron energy over an energy interval of some 20–30 eV. Therefore, in the wave crests, ionisation of the neutral gas will proceed at a rate larger than in the wave troughs and the wave might grow if the damping mechanisms which are present are not too strong.

We can analyse this growth mechanism by treating ions and electrons as fluids of nearly the same densities (charge quasineutrality). We also assume Boltzmann equilibrium for the electrons ($\kappa T_e \nabla n = en\nabla\varphi$, where T_e is the electron temperature, n the plasma density, φ the electric potential, κ Boltzmann's constant and e the electron charge). We take the ions to be much colder than the electrons ($T_i \ll T_e$) and write the ion continuity and momentum equations in one dimension as

$$\frac{\partial n}{\partial t} + \frac{\partial}{\partial z}(nv) + \frac{n}{\tau_L} - Q = 0 \tag{1}$$

$$nm\frac{\partial v}{\partial t} + nmv\frac{\partial v}{\partial z} + en\frac{\partial \varphi}{\partial z} + \nu nmv - nm\beta\nabla^2 v + Qmv = 0. \tag{2}$$

In equation (1) the term n/τ_L accounts for whatever ion losses may be present (generally the most important are transport losses across the confining magnetic field) with a loss time τ_L. Q represents the rate of production of new ions by ionisation. Thus

$$Q = \sigma_I N\Phi \tag{3}$$

where σ_I is the ionisation cross section, N the neutral gas density and Φ the flux of ionising electrons. The density of the fast, ionising electrons is in general much smaller than the density of the thermal electrons whose density is thus nearly equal to that of the ions.

In equation (2), the term νnmv represents momentum losses by the ions through collisons with the neutral gas with the collision frequency ν. The term Qmv accounts for the fact that a sink term in the ion momentum equation must arise if the new ions produced by ionisation have an average velocity different from the instantaneous velocity of the ion fluid. This same term was also retained by D'Angelo (1967) in analysing a recombination instability. The term $-nm\beta\nabla^2 v$ represents the effect of viscosity, where β is the kinematic viscosity coefficient.

To account for the variation of the ionisation cross section with electron energy, we assume that σ_I in equation (3) can be written as

$$\sigma_I = \sigma_0 + \left(\frac{d\sigma_I}{d\varphi}\right)_0 d\varphi \tag{4}$$

where σ_0 represents some value of the ionisation cross section slightly above the threshold. The expansion of σ_I in terms of the electron energy retains only the linear term. This should be quite adequate in the linearised treatment of the waves presented below.

Equations (1) and (2) are linearised around a zero-order state with $\partial/\partial t \equiv 0$, $v \equiv v_0 \equiv 0$, $\varphi \equiv \varphi_0 \equiv 0$ and $\partial/\partial z \equiv 0$. In this state

$$n_0/\tau_L = \sigma_0 N\Phi. \tag{5}$$

Equation (5) relates the time loss τ_L to the zero-order plasma density n_0 and the rate of production of new ions by ionisation.

Linearisation of equations (1) and (2) is performed in the usual manner and the space and time variation of the first-order quantities is taken to be of the type $\exp i(Kz - \omega t)$, where K is the wave number and ω is the angular frequency.

A dispersion relation is then easily arrived at, which reads

$$\omega^2 + i\left[\nu + \beta K^2 + \frac{2}{\tau_L} - \left(\frac{d\sigma}{d\varphi}\right)_0 \frac{N\Phi}{n_0}\frac{\kappa T_e}{e}\right]\omega - \left[\frac{1}{\tau_L} - \left(\frac{d\sigma}{d\varphi}\right)_0 \frac{N\Phi}{n_0}\frac{\kappa T_e}{e}\right]\left(\nu + \beta K^2 + \frac{1}{\tau_L}\right) - K^2 C_s^2 = 0 \tag{6}$$

where $C_s = (\kappa T_e/m)^{1/2}$ is the ion-acoustic speed. Next we take the wave number K to be real and the frequency ω to be complex with $\omega = \omega_r + i\gamma$. A positive value of the growth rate γ corresponds to wave growth, a negative γ to wave damping. The dispersion relation, equation (6), can be separated into real and imaginary parts and with a little algebra gives

$$\omega_r^2 = K^2 C_s^2 - \left(\gamma + \nu + \beta K^2 + \frac{1}{\tau_L}\right)^2 \tag{7}$$

$$\gamma = \tfrac{1}{2}\left[\frac{1}{\tau_L}\left(\frac{\Delta\sigma}{\sigma_0} - 1\right) - \left(\nu + \beta K^2 + \frac{1}{\tau_L}\right)\right] \tag{8}$$

where $\Delta\sigma = [d\sigma_I/d(e\varphi)]_0 \kappa T_e$.

It is evident from equation (8) that a positive growth rate can be obtained only if the increase of the ionisation cross section with electron energy is sufficiently rapid to overcome the damping effects of collisions, viscosity and ion losses. Equation (7) shows

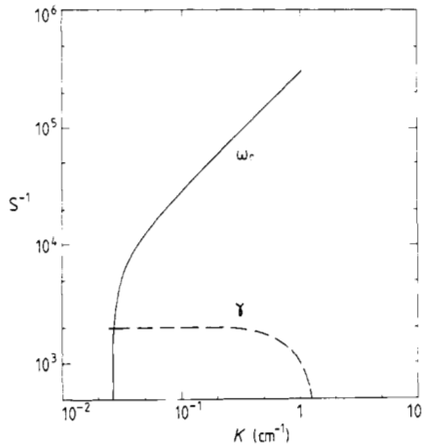

Figure 4. The ionisation instability. The wave angular frequency ω_r and the growth rate γ against the wave number K. The calculations were performed for $1/\tau_L = 10^3\,s^{-1}$, $(\Delta\sigma/\sigma_0 - 1) = 10$, $\nu = 5 \times 10^3\,s^{-1}$, $\beta/\nu = 0.4\,cm^2$ and $C_s = 3 \times 10^5\,cm\,s^{-1}$.

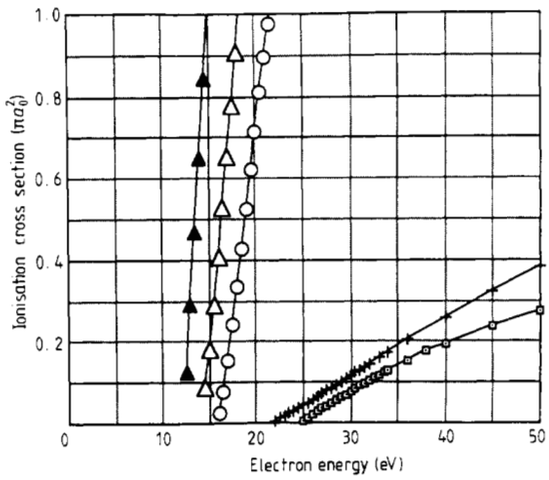

Figure 5. Ionisation cross section against electron energy for ⊡, He; +, Ne; ○, Ar; △, Kr and ▲, Xe (from Rapp and Englander-Golden 1965).

that the waves are, in fact, ordinary ion-acoustic waves. However, it also shows that no propagating modes exist at very low K number, where ω_r^2 becomes negative, nor at very large K number because of viscosity. As an example of the solution provided by equations (7) and (8) figure 4 shows ω_r and γ as functions of K for $1/\tau_L = 10^3\,s^{-1}$, $(\Delta\sigma/\sigma_0 - 1) = 10$, $\nu = 5 \times 10^3\,s^{-1}$, $\beta/\nu = 0.4\,cm^2$ and $C_s = 3 \times 10^5\,cm\,s^{-1}$.

5. Discussion and conclusions

The properties of the low-frequency oscillations summarised in § 3 ((i)–(iv)) suggest that we have observed ion-acoustic waves excited by an ionisation instability of the type examined in § 4.

The calculations of § 4 predict frequencies below a few kilohertz for wavelengths comparable to the length of the 'system', i.e. to the axial distance between grid and DL (property (i)). The excitation mechanism of § 4 requires relatively high gas pressures and the presence of fast electrons which are energetic enough to ionise the neutral gas (properties (ii) and (iii)). Finally, it is possible to understand why the instability is most easily excited in xenon gas, is also easily seen in krypton and argon, but never in neon or helium. Figure 5 shows the ionisation cross section against electron energy in the range 0–50 eV for He, Ne, Ar, Kr and Xe. These data are taken from the work of Rapp and Englander-Golden (1965). The most rapid variation of σ_I with electron energy $e\varphi$ occurs for Xe; Kr is next, followed by Ar. The two lighter gases, Ne and He, show a much smaller $d\sigma_I/d(e\varphi)$. Thus, according to equation (8), the growth rate for these last two gases may be negative under practically all circumstances.

Numerical results of the type shown in figure 4 indicate that ion viscosity is probably the agent responsible for setting an upper limit to the frequency of observable waves. They also indicate that a linear theory developed for a uniform plasma with no boundaries allows waves to be excited with frequencies extending all the way from this upper limit down to zero frequency. Thus, one might expect a continuous frequency spectrum from 0 Hz to the upper limit set by ion viscosity instead of a narrow frequency band. It seems possible that non-linearities and the finite size of the system may be responsible for concentrating the oscillation energy into wavelengths comparable with the system size.

Ion-acoustic waves and ionisation waves often have similar frequencies (Pekarek 1971). Ionisation instabilities have been considered before in the literature (e.g. Akhiezer *et al* 1970). Together with, e.g. the recombination instability, they belong to a more general class of plasma instabilities where overall density changes are caused by volumetric processes (Kofoed-Hansen 1969).

Acknowledgments

We wish to thank Al Scheller for his expert technical assistance. This work was supported by ONR and NASA.

References

Akhiezer A I, Akhiezer I A and Angeleiko V V 1970 *Sov. Phys.–JETP* **30** 476
D'Angelo N 1967 *Phys. Fluids* **10** 719
Johnson J C, Merlino R L and D'Angelo N 1989 *J. Phys. D: Appl. Phys.* **22** 1456
Kofoed-Hansen O 1969 *Phys. Fluids* **12** 2141
Pekarek L 1971 *Xth Int. Conf. on Phenomena in Ionized Gases (Oxford)* invited paper, ed P A Davenport (Oxford: Parsons) pp 365–403
Rapp D and Englander-Golden P 1965 *J. Chem. Phys.* **43** 1464